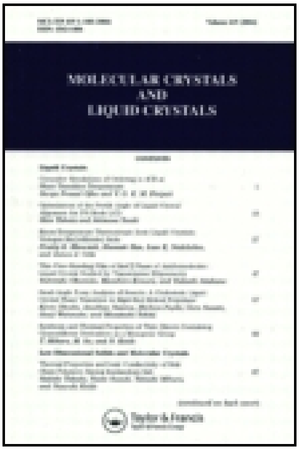

Molecular Crystals and Liquid Crystals Science and Technology. Section A. Molecular Crystals and Liquid Crystals

Publication details, including instructions for authors and subscription information:
http://www.tandfonline.com/loi/gmcl19

Influence of Structural Isomerism on the Electronic Properties of Extended Phthalocyanines

E. Ortí [a], M. C. Piqueras [a], R. Crespo [a] & F. Tomás [a]

[a] Departament de Química Física, Universitat de València, Dr. Moliner 50, E-46100, Burjassot, Valencia, Spain

Version of record first published: 04 Oct 2006.

To cite this article: E. Ortí , M. C. Piqueras , R. Crespo & F. Tomás (1993): Influence of Structural Isomerism on the Electronic Properties of Extended Phthalocyanines, Molecular Crystals and Liquid Crystals Science and Technology. Section A. Molecular Crystals and Liquid Crystals, 234:1, 241-246

To link to this article: http://dx.doi.org/10.1080/10587259308042922

Mol. Cryst. Liq. Cryst. 1993, Vol. 234, pp. 241–246
Reprints available directly from the publisher
Photocopying permitted by license only

Printed in the United States of America

INFLUENCE OF STRUCTURAL ISOMERISM ON THE ELECTRONIC PROPERTIES OF EXTENDED PHTHALOCYANINES

E. ORTÍ, M.C. PIQUERAS, R. CRESPO and F. TOMÁS
Departament de Química Física, Universitat de València
Dr. Moliner 50, E-46100 Burjassot, Valencia (Spain)

Abstract The electronic structure of isomeric naphthalocyanines (H_2Nc) is investigated using the nonempirical valence effective Hamiltonian (VEH) technique. The way the outer benzene rings are annelated (linearly as in 2,3-H_2Nc or angularly as in 1,2-H_2Nc) is shown to determine very important changes in the electronic properties. While similar properties to those of phthalocyanine are calculated for 1,2-H_2Nc, lower oxidation potentials and red-shifted optical absorptions are predicted for 2,3-H_2Nc in agreement with experimental data. The isomerism resulting from the different relative positions of the angularly annelated benzene rings in 1,2-H_2Nc is shown to have almost no effect on the electronic properties.

INTRODUCTION

Besides their traditional uses as dyes, pigments, and catalysts, phthalocyanines (Pc) are of particular interest in many fields of basic and applied research as molecular units to build up electroresponsive materials[1,2]. Applications of phthalocyanines in electronics, optoelectronics, and molecular electronics are very large and concern diverse fields such as energy conversion cells, gas sensors, low-dimensional metals, electrochromic devices, optical data recording, liquid crystals, LB films, and nonlinear optics.

The unique electrical and optical properties that phthalocyanines exhibit are mainly determined by the large π-electronic system that characterizes these compounds. Phthalocyanines consist of a 42 π-electrons conjugated system delocalized over the forty carbon and nitrogen atoms forming the planar macrocycle. The enlargement of this conjugated macrocycle is therefore expected to improve the optical and electronic properties of phthalocyanines. Many synthetic efforts have recently been devoted to obtain extended phthalocyanine-based compounds such as naphthalocyanines[3,4], phenanthrenocyanines[5,6] and anthracenocyanines[7].

In this paper we focus on the electronic properties of naphthalocyanines (Nc). Comparing to phthalocyanines, these compounds exhibit high electrical conductivities 10^{-5}-10^{-3} S/cm) without any external doping[3] and strong absorption bands in the nearinfrared[8,9]. These properties have been shown to be strongly dependent of the molecular structure of the naphthalocyanine molecule which presents different isomers depending on the way the outer benzene rings are annelated, linearly as in 2,3-Nc or angularly as in 1,2-Nc (see Fig. 1). While 2,3-NcFe and $[2,3\text{-NcFe(dib)}]_n$ compounds show powder conductivities of $\sigma_{RT}=4 \times 10^{-5}$ and 4×10^{-3} S/cm, respectively, 1,2-NcFe and $[1,2\text{-NcFe(dib)}]_n$ exhibit almost insulating properties ($\sigma_{RT}=4 \times 10^{-9}$ and 6×10^{-10} S/cm, respectively)[4].

Our main goal in this paper is to rationalize how the electronic properties of naphthalocyanine compounds can be modulated by varying the isomer structure. We present the results of valence effective Hamiltonian (VEH) theoretical calculations on the electronic structure of metal-free 2,3 naphthalocyanine (2,3-H_2Nc) and 1,2-naphthalocyanine (1,2-H_2Nc) (see Figure 1). The electronic properties of 2,3-H_2Nc and 1,2-H_2Nc were previously investigated using the VEH method[10,11]. For 1,2-H_2Nc, we study how the relative position of the outer benzene rings on adjacent isoindole rings affects the electronic structure of the macrocycle. The four isomers depicted in Figure 2 and named 1,2-A to 1,2-D are obtained when synthesizing 1,2-naphthalocyanines[4,12]. The VEH method is well documented in the literature[13] and has been successfully applied to the study of phthalocyanine compounds[10,11,14,15]. This method is especially useful in dealing with very large molecular systems since it is completely nonempirical and yields one-electron energies of ab initio double-zeta quality at a reasonable computer cost.

RESULTS AND DISCUSSION

Geometric Structures

The geometries optimized for the 2,3-H_2Nc and 1,2-H_2Nc molecules using the MNDO-PM3 (modified neglect of diatomic overlap, parametric method 3) semiempirical method[16] are displayed in Figure 1. The geometry of 2,3-H_2Nc has been calculated assuming that the molecule is totally planar and has D_{2h} symmetry. The geometries of 1,2-A to 1,2-D have been obtained by preserving the structure obtained for the tetraazaporphyrin ring in 2,3-H_2Nc and optimizing the outer naphthalene units under the respective symmetry constraint (C_{2h} or C_s). Only the geometry obtained for 1,2-A is depicted in Figure 1 since almost no changes are calculated for isomers 1,2-B to 1,2-D. Bond lengths are affected by less than 0.001 Å and bond angles by less that 0.2°.

The alternant structure of localized single and double bonds drawn in Figure 1 for 2,3-H_2Nc provides a misleading picture of the molecular structure of this compound. Figure 3 compares the geometry found for a naphthopyrrole moiety in 2,3-H_2Nc with the PM3-optimized geometries of isoindole, pyrrole, and naphthalene molecules. There are marked differences between the geometry of the pyrrole units within naphthalocyanine and those in isoindole and pyrrole molecules. For pyrrole, the C_α-C_β atoms are joined by bonds showing a high degree of double-bond character (1.390 Å). The structure of pyrrole is mainly retained in the isoindole molecule (C_α-C_β=1.405 Å), which can be considered as resulting from the fusion of a pyrrole ring with 1,3-butadiene. The situation is opposite in naphthalocyanine where the C_α-C_β bonds have mostly single-bond character

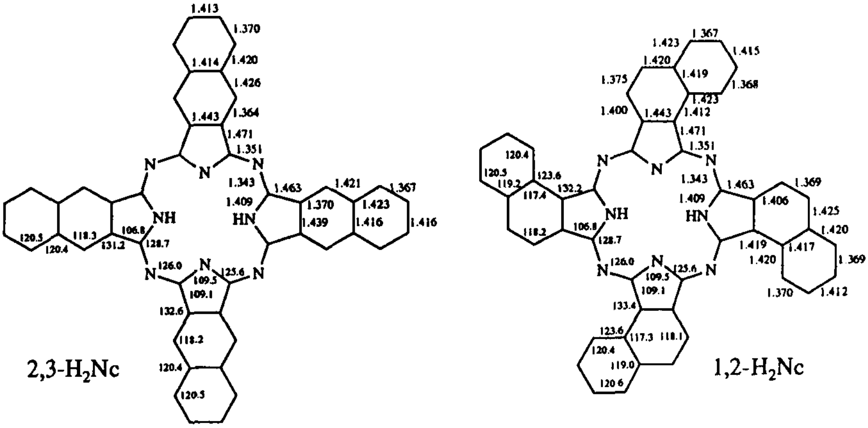

FIGURE 1 Molecular structures and PM3-optimized parameters for 2,3-naphthalocyanine (2,3-H$_2$Nc) and 1,2-naphthalocyanine (1,2-H$_2$Nc). Bond lengths are in Å and bond angles in degrees.

(1.463 Å) and the two benzene ring have a geometry almost identical to that of naphthalene (see Figure 3). Thus, the geometry of pyrrole is not preserved in naphthalocyanines which have to be visualized as the result of joining four naphthalene units to the central carbon-nitrogen methineimine-like macrocycle. This conclusion is supported from an electronic structure standpoint, since the phtoemission bands appearing in the experimental photoelectron spectrum of naphthalocyanine show a one-to-one correspondence with those observed for naphthalene[19].

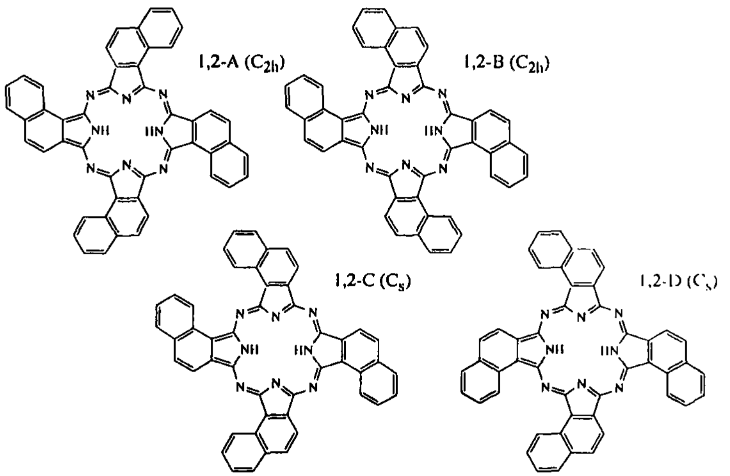

FIGURE 2 Constitutional isomers of 1,2-H$_2$Nc and their point group symmetries.

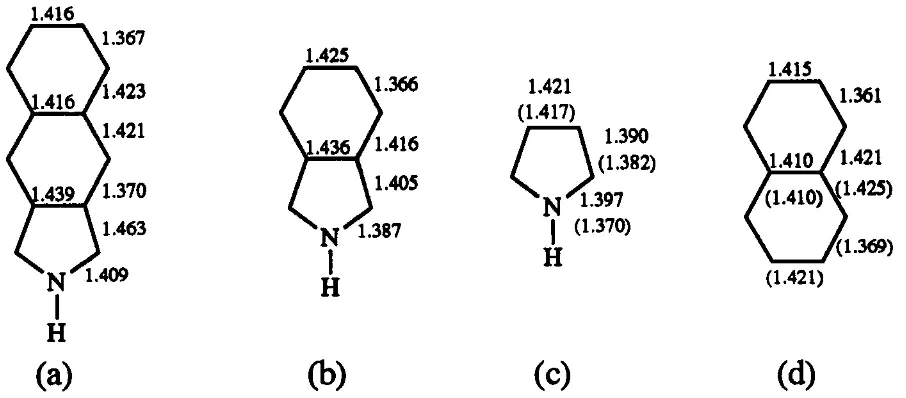

FIGURE 3 Comparison of PM3-optimized bond lengths (in Å) of pyrrole and related compounds: (a) naphthopyrrole units in 2,3-H_2Nc; (b) isoindole molecule; (c) pyrrole molecule (experimental microwave data in parentheses[17]); (d) naphthalene molecule (experimental UV absorption data (rotational structure) in parentheses[18]).

Electronic Structures

Table I summarizes the highest occupied and lowest unoccupied molecular orbital distributions obtained for 2,3-H_2Nc and 1,2-H_2Nc using the VEH method. The one-electron energy levels calculated for phthalocyanine (H_2Pc) are also included for the sake of comparison. The molecular orbitals have been classified according to the D_{2h} point group of symmetry except for 1,2-naphthalocyanine isomers which assume a C_{2h} structure. The energies collected in Table I differ from those previously reported[10] due to the geometric parameters used to define the molecular structures. In the previous work[10], we built up the geometries of H_2Pc and 2,3-H_2Nc from average neutron diffraction data on H_2Pc[20] and that of 1,2-H_2Nc from X-ray diffraction data on 1,2-NcFe(RCN)$_2$[4]. Here, we make use of the PM3-optimized geometries discussed above for 2,3-H_2Nc and 1,2-H_2Nc. The geometry of H_2Pc has been also optimized using the PM3 method and a D_{2h} symmetry constraint.

The $4a_u$ HOMO of phthalocyanine is calculated at an energy of -6.42 eV in perfect agreement with the first ionization potential (6.41 eV) reported from gas-phase UPS measurements on H_2Pc[21]. An energy destabilization of the HOMO is obtained when passing to 2,3-H_2Nc for which the $6a_u$ HOMO is calculated to lie at -6.05 eV (0.37 eV above the HOMO of H_2Pc). Since oxidation involves removing an electron from the HOMO, the relative stabilities of the HOMO levels predicted by the VEH method justify the lower oxidation potentials measured for 2,3-naphthalocyanine compounds compared to those observed for phthalocyanines[12,22]. In contrast to 2,3-H_2Nc, the angular condensation of benzene rings to obtain 1,2-H_2Nc produces a stabilization of the HOMO level which is now located at -6.70 eV. The higher conductivities observed for 2,3-naphthalocyanine compounds could therefore be explained as due to the low oxidation potential of the macrocycle, which renders oxidative doping with air oxygen possible[3,23].

TABLE I VEH one-electron energy levels (ε_i, in eV) obtained for phthalocyanine (H_2Pc), 2,3-naphthalocyanine (2,3-H_2Nc), and 1,2-naphthalocyanine (1,2-H_2Nc-A and B)[a].

H_2Pc		2,3-H_2Nc		1,2-H_2Nc-A		1,2-H_2Nc-B	
$5a_u^*$	-4.01	$10b_{1u}$	-4.27	$16a_u$	-4.65	$16a_u$	-4.65
$6b_{2g}^*$	-5.16	$8b_{2g}^*$	-5.00	$16b_g$	-5.49	$16b_g$	-5.49
$6b_{3g}^*$	-5.23	$8b_{3g}^*$	-5.02	$15b_g$	-5.54	$15b_g$	-5.55
$4a_u$	-6.42	$6a_u$	-6.05	$15a_u$	-6.70	$15a_u$	-6.70
$7b_{1u}$	-9.39	$5a_u$	-8.57	$14a_u$	-8.45	$14a_u$	-8.43
$5b_{2g}$	-9.42	$7b_{3g}$	-8.65	$14b_g$	-8.48	$14b_g$	-8.45
$5b_{3g}$	-9.43	$7b_{2g}$	-8.66	$13a_u$	-8.49	$13a_u$	-8.52
$6b_{1u}$	-9.43	$4a_u$	-8.96	$13b_g$	-8.49	$13b_g$	-8.52
$3a_u$	-9.64	$9b_{1u}$	-9.22	$12a_u$	-9.34	$12a_u$	-9.33

[a] The highest six occupied and the lowest three unoccupied levels are included. All orbitals are of π-nature.

In that which concerns the optical properties, a narrowing of the HOMO-LUMO energy gap is observed in going from H_2Pc (1.78 eV) to 2,3-H_2Nc (1.62 eV). This narrowing explains the red shift observed for the longest-wavelength optical absorption (band Q) in passing from H_2Pc to 2,3-H_2Nc[7]. The tetra-*tert*-butylated derivative of H_2Pc shows two intense absorption peaks at 698 and 664 nm in pyridine solution which are in perfect correlation with the $4a_u \rightarrow 6b_{2g}^*$ (697 nm) and $4a_u \rightarrow 6b_{3g}^*$ (671 nm) electronic transitions predicted by the VEH method. The same derivative of 2,3-H_2Nc presents a unique absorption peak at 784 nm[7] in good agreement with theoretical predictions. The $15b_g^*$ and $16b_g^*$ MOs are almost degenerate ($\Delta\varepsilon_i$=0.02 eV) and an electronic transition about 765 nm is obtained.

Although the HOMO of 1,2-H_2Nc is stabilized by 0.28 eV with respect to the HOMO of H_2Pc, the LUMO is also stabilized in a similar amount (0.31 eV) and, in contrast to 2,3-H_2Nc, the HOMO-LUMO energy gap remains almost constant in going from H_2Pc (1.78 eV) to 1,2-H_2Nc (1.75 eV). This result is supported by the almost equal wavelengths experimentally reported for octahedrally complexed iron derivatives of H_2Pc (658 nm) and 1,2-H_2Nc (653 nm)[23].

As can be seen from Table I, the electronic structure of 1,2-H_2Nc is not affected by the different relative positions of the outer benzene rings giving rise to the constitutional isomers depicted in Figure 1. Table I only collects the MO distributions obtained for 1,2-A and 1,2-B, which are the isomers showing the most important structural differences. The one-electron energies calculated for these two isomers differ by less than 0.05 eV and this is also the case when comparing with 1,2-C and 1,2-D.

In conclusion, naphthalocyanine must be viewed from both the geometric and electronic structure standpoints as the result of joining four naphthalene units to the central carbon-nitrogen macrocycle. The optical and electronic properties calculated for 2,3-H_2Nc and 1,2-H_2Nc show clearly different trends when compared to those of H_2Pc

and suggest the possibility of monitoring the properties of phthalocyanine-based electroresponsive materials by changing the structure of the macrocycle. No relevant difference is found for the electronic properties of 1,2-H_2Nc isomers.

ACKNOWLEDGEMENTS

We thank the Servei d'Informàtica de la Universitat de València for the use of their computing facilities. M.C.P. and R.C. are grateful to the Ministerio de Educación y Ciencia of Spain for a Doctoral Grant. This work has been supported by the Generalitat Valenciana and the DGYCIT Projects PS88-0112 and OP90-0042. We are indebted to Prof. N. Kobayashi for communicating unpublished data on naphthalocyanines.

REFERENCES

1. A.B.P. Lever, M.R. Hempstead, C.C. Leznoff, W. Liu, M. Melnik, W.A. Nevin and P. Seymour, Pure Appl. Chem., 58, 1467 (1986); C.C. Leznoff and A.B.P. Lever (eds.), Phthalocyanines: Properties and Applications (VCH, New York, 1989).
2. T.J. Marks, Angew. Chem. Int. Ed. Engl., 29, 857 (1990).
3. S. Deger and M. Hanack, Synth. Met., 13, 319 (1986); Isr. J. Chem., 27, 347 (1986).
4. M. Hanack, G. Renz, J. Strähle and S. Schmid, Chem. Ber., 121, 1479 (1988).
5. A.W. Snow and T.R. Price, Synth. Met., 9, 329 (1984).
6. M. Hanack and G. Renz, Chem. Ber., 123, 1105 (1990).
7. N. Kobayashi, S. Nakajima and T. Osa, personal communication.
8. M.L. Kaplan, A.J. Lovingen, W.D. Reents, Jr. and P.H. Schmidt, Mol. Cryst. Liq. Cryst., 112, 345 (1984).
9. Y. Iwakabe, S. Numata, N. Kinjo and A. Kakuta, Bull. Chem. Soc. Jpn., 63, 2734 (1990).
10. E. Ortí, M.C. Piqueras, R. Crespo and J.L. Brédas, Chem. Mater., 2, 110 (1990).
11. E. Ortí, M.C. Piqueras, R. Crespo and J.L. Brédas, Synth. Met., 42, 2647 (1990).
12. M. Hanack, G. Renz, J. Strähle and S. Schmid, J. Org. Chem., 56, 3501 (1991).
13. J.M. André, J.L. Brédas, J. Delhalle, D.J. Vanderveken, D.P. Vercauteren and J.G. Fripiat, in MOTECC-90 (Modern Techniques in Computational Chemistry, edited by E. Clementi (ESCOM, Leiden, 1990), Chap. 15, p. 745.
14. E. Ortí and J.L. Brédas, J. Chem. Phys., 89, 1009 (1988).
15. E. Ortí, J.L. Brédas and C. Clarisse, J. Chem. Phys., 92, 1228 (1990).
16. J.J.P. Stewart, J. Comput. Chem., 10, 209 (1989); 10, 221 (1989).
17. L. Nygaard, J.J. Nielsen, J. Kirchheiner, G. Maltesen, J. Rastrup-Andersen and G.O. Sorensen, J. Mol. Struct., 3, 491 (1969).
18. K.K. Innes, J.E. Parkin, D.K. Ervin, J.M. Hollas and J.G. Ross, J. Mol. Spectrosc., 16, 406 (1965).
19. E. Ortí, R. Crespo, M.C. Piqueras, P.M. Viruela and F. Tomás, Synth. Met., in press.
20. B.F. Hoskins, S.A. Mason and J.C.B. White, J. Chem. Soc., Chem. Commun., 554 (1969).
21. J. Berkowitz, J. Chem. Phys., 70, 2819 (1979).
22. M. Hanack, A. Hirsch, A. Lange, M. Rein, G. Renz and P. Vermehren, J. Mater. Res., 6 (1991) 385.
23. M. Hanack, A. Lange, M. Rein, R. Behnisch, G. Renz and L. Leverenz, Synth. Met., 29, F1 (1989).
24. For the sake of consistency, HOMO-LUMO energy gaps are calculated by adding 0.59 eV as in previous works (ref. 10, 11 and 15). This is to correct for the too small energy gap that the VEH method predicts for H_2Pc.